

Citation for published version:

Nikolay Dimov, et al, 'Solvent-selective routing for centrifugally automated solid-phase purification of RNA', *Microfluidics and Nanofluidics*, Vol. 18 (5-6): 859-871, May 2015.

DOI:

<https://doi.org/10.1007/s10404-014-1477-9>

Document Version:

This is the Accepted Manuscript version.

The version in the University of Hertfordshire Research Archive may differ from the final published version.

Copyright and Reuse:

© 2014 by Springer Berlin Heidelberg.

This manuscript version is made available under the terms of the Creative Commons Attribution licence (<http://creativecommons.org/licenses/by/4.0/>), which permits unrestricted re-use, distribution, and reproduction in any medium, provided the original work is properly cited.

Enquiries

If you believe this document infringes copyright, please contact the Research & Scholarly Communications Team at rsc@herts.ac.uk

Solvent-selective routing for centrifugally automated solid-phase purification of RNA

Nikolay Dimov · Eoin Clancy · Jennifer Gaughran · David Boyle · Darren Mc Auley · Macdara T. Glynn · Róisín M. Dwyer · Helena Coughlan · Thomas Barry · Louise Barrett · Terry J. Smith · Jens Ducreé

Received: date / Accepted: date

Abstract We present a disc-based module for rotationally controlled solid-phase purification of RNA from cell lysate. To this end, multi-stage routing of a sequence of aqueous and organic liquids into designated waste and elution reservoirs is implemented by a network of strategically placed, solvent-selective composite valves. Using a bead-based stationary phase at the entrance of the router, we show that total RNA is purified with high integrity from cultured MCF7 and T47D

cell lines, human leukocytes and *Haemophilus influenzae* cell lysates. Furthermore, we demonstrate the broad applicability of the device through the *in vitro* amplification of RNA purified on-disc using RT-PCR and NASBA. Our novel router will be at the pivot of a forthcoming, fully integrated and automated sample preparation system for RNA-based analysis.

Keywords Lab-on-a-disc · RNA purification · Solvent-selective valves · Molecular diagnostics

Nikolay Dimov
Biomedical Diagnostics Institute, National Centre of Sensor Research, School of Physical Sciences, Glasnevin, Dublin 9, Ireland
E-mail: n.dimov@ucl.ac.uk

Eoin Clancy · Helena Coughlan · Thomas Barry · Terry J. Smith
School of Natural Sciences, Biomedical Diagnostics Institute Programme, National Centre for Biomedical Engineering Science, National University of Ireland, Galway, Ireland

Jennifer Gaughran · David Boyle · Darren Mc Auley · Macdara T. Glynn · Louise Barrett
Biomedical Diagnostics Institute, National Centre of Sensor Research, School of Physical Sciences, Glasnevin, Dublin 9, Ireland

Róisín M. Dwyer
School of Medicine, National University of Ireland, Galway, Ireland

Jens Ducreé
Biomedical Diagnostics Institute, National Centre of Sensor Research, School of Physical Sciences, Glasnevin, Dublin 9, Ireland
Fax: +353 1 700 7870
Tel: +353 1 700 5377
E-mail: jensducree@dcu.ie

1 Introduction

Microfluidic lab-on-a-chip technologies have been shown to automate and reduce the time-to-result of a wealth of bioanalytical assays, and ultimately enable their deployment at the point of need. Whilst a range of detection techniques remains implemented on-chip, the integration of sample preparation with detection has been a bottleneck in the development of microfluidic devices for nucleic acid testing (Foudeh *et al.*, 2012; McCalla and Tripathi, 2011). In many instances, RNA is a preferable diagnostics target, such as the detection of retro viruses or in the expression analysis of genes. Also, in assays for the detection of pathogens, RNA can be used to obtain information on pathogen viability as RNA is less stable than the DNA. Furthermore, since RNA molecules are typically present in multi-copy (100s-1000s/per cell), the potential for detection without *in vitro* enzymatic amplification is possible. One such class of RNA species that have recently received attention for their diagnostic potential are micro-RNAs (miRNAs). miRNAs are small non-coding RNAs that are involved in modulating gene expression at the transcriptional and post transcriptional

level. Their dysregulation has been shown to be associated with a wide variety of human diseases, including cancer (Mitchell *et al.*, 2008; Heneghan *et al.*, 2010), diabetes and cardiovascular diseases. In terms of bacterial RNA diagnostics, ribosomal RNA (rRNA) and in particular 16S rRNA remains the gold standard. Other functional high-copy number bacterial RNA molecules such as transfer messenger RNA (tmRNA) encoded by the *ssrA* gene has been demonstrated to be a useful marker in bacterial diagnostics (O'Grady *et al.*, 2009; Clancy *et al.*, 2012).

The automation of microfluidic platforms often involves the use of costly peripheral equipment, such as syringe pumps, external valves and pressure controllers. These chip in a lab devices require complex, multi-stage off-chip liquid handling steps, thereby severely limiting their wide spread adoption in clinical testing. Centrifugal microfluidic Lab-on-a-Disc (LoaD) systems bear the potential to integrate sample preparation with detection to create full-fledged sample-to-answer devices (Madou *et al.*, 2006; Ducrée *et al.*, 2007). A simple rotary microsystem developed by Park *et al.* (2012a), enabled the purification of RNA from viral lysate with frequency controlled release of reagents. Using centrifugal micro-fluidics, Cho *et al.* presented a device capable of one-step DNA extraction of pathogen-specific DNA from whole blood (Cho *et al.*, 2007). Also multiplexing of immunoassays on-disc (Lee *et al.*, 2009; Park *et al.*, 2012) and parallelized biochemical analysis (Lee *et al.*, 2011) have been demonstrated.

As all liquids resident on the disc are simultaneously exposed to the same centrifugal field, valving technologies are pivotal for establishing a sequence of liquid handling steps. Over the years the scientific community has pioneered a repertoire of valving schemes, which are commensurate with the rotational nature of the lab-on-a-disc platform. Amongst the central aspects governing the choice of the valving scheme are the upper limit of tolerable spin frequencies (e.g. during *multi-stage* sample prep), the open-state hydrodynamic resistance and vapour barrier properties (e.g. for storage and release of liquid reagents) on behalf of flow control and the complexities involved in fabrication and actuation on the hardware side. Valve actuation on LoaD platforms can be categorized into two schemes; the first type of valve is controlled by the system-innate spindle motor such as capillary burst valves (Ducrée *et al.*, 2007; Zoval and Madou, 2004) or siphons (Schembri *et al.*, 1995; Steigert *et al.*, 2007; Nwankire *et al.*, 2013); the alternative, externally actuated schemes often involve the manipulation of a sacrificial material by an external stimulus like heat, for instance, thermally-actuated wax valves (Park *et al.*, 2007). Recent reports have uti-

lized such wax valves for the on-disc integration of biochemical and immunoassays (Lee *et al.*, 2009, 2011). To avoid the manufacturing complexity of incorporating on-disc heat induced valves, Mark *et al.* (2008) introduced a pneumatic microvalve using a thin burstable foil. Zehnle *et al.* (2012) swiftly balance the pressures on spinning disc, and use the advancing liquid as a valve to achieve inward pumping. In another study, Gorkin III *et al.* (2012) integrated water-dissolvable films as once-off valve seals. By trapping air between this dissolvable film and the liquid they implemented centrifugo-pneumatic valving and gating of on-board-stored reagents for a wide range of burst frequencies. We expand upon these dissolvable film valves and develop automated, solvent-selective routing on a LoaD platform.

For solid-phase purification (SPP) of nucleic acids, we here exploit the well-established Boom chemistry (Boom *et al.*, 1990). Fluidic routing to direct flow to a selected output at a bifurcation between a waste and an elution outlet is critical for centrifugally implemented automation. Kim *et al.* (2008) developed a flow switch by using a capillary valve upstream of an open chamber and unique 3D junction geometry. A similar router, solely controlled by the rotationally actuated hydrodynamic Coriolis pseudo force, was reported by Brenner *et al.* (2005). This virtual routing concept was further sophisticated by Haeberle *et al.* (2007) who successfully extracted DNA from calf thymus using silica beads by alternating the sense of rotation. Based on a droplet deflection Coriolis-force driven router they recovered 16% of the initial nucleic acid. A recent study by Seo reports 81% capture efficiency of RNA from lysed influenza A H3N2 virus using silane, *i.e.* TEOS treated glass beads on-disc (Seo *et al.*, 2013). Alternatively, 100% efficient automated extraction of human genomic DNA is demonstrated by Kloke *et al.* (2014) who implement novel ball-pen piercable seals to route the sample lysate through integrated silica membrane in a Lab Tube platform. Whilst these systems have contributed greatly to the development of SPP, to date, reliable, high-efficiency and low-complexity routing of flows (e.g. aqueous or organic flows) on LoaD platforms still remains a challenge.

We report a routing scheme which utilizes solvent-selective valving with unidirectional rotational actuation for SPP of RNA, thereby obviating the need for external actuation other than the system-inherent spinning rates. Previously Kinahan *et al.* (2014) successfully achieved solid phase purification of total RNA from MCF7 cell lysates. Multiple dissolvable film valving strategies were presented, which allowed inbuilt control of reagent release for automated sample preparation and integration of laboratory unit operations on

LoadD at constant angular velocity. However, the article briefly touches on the quality of the purified samples and the mechanisms of routing. In contrast, here we investigate solid phase purification of RNA from various cells, study the suitability of the method for further downstream amplifications, and expand on the selective routing through integrated hydrophobic membrane and dissolvable film valves. Our findings will be at the core of a future, fully automated centrifugal microfluidic nucleic acid analyzer.

2 Principle of operation

This paper addresses the missing link between upstream, chemically induced cell lysis and 3-phase RNA extraction and downstream nucleic acid analysis techniques which are both well established bench-top methods that have also been demonstrated microfluidically using lab-on-a-chip / lab-on-a-disc systems (Linares *et al.*, 2011). The single step acid guanidinium thiocyanate phenol-chloroform method, also known as 3-phase RNA extraction, is based on the discovery that RNA (other than DNA and proteins) remains soluble in the acidic aqueous phase (Brenner *et al.*, 2005; Chomczynski and Sacchi, 1987). Formulations of acidic guanidinium thiocyanate and phenol are commercially available under various brand names (TRIzol from LifeTechnologies, TRI Reagent from Sigma). In general, the reagent contains phenol that ruptures the cells and guanidinium thiocyanate, a chaotropic salt that strips protein complexes from RNA. The addition of chloroform (or an alternative reagent such as 4-bromoanisole or 1-Bromo-3-chloropropane), prior to centrifugation permits the separation of the non-polar (organic) and polar (aqueous) phases. Due to differences in their solubility, DNA is retained in the organic phase whilst the RNA is concentrated in the aqueous phase, which also contains salt contamination. For accurate downstream analysis of RNA, it is essential that extracted RNA is free of contaminants such as chaotropic salts and phenol (Bustin and Nolan, 2004; Tan and Yiap, 2009).

Here we convey the centrifugal microfluidic automation of a 4-stage purification of RNA from the aqueous phase of TRI Reagent lysed human and bacterial cells. Using human MCF7 breast cancer cells, we validate the device. Subsequently, we demonstrate the applicability of the device for nucleic acid diagnostics with the *in vitro* enzymatic amplification of miRNAs from cultured T47D cells and human leucocytes using RT-PCR. Furthermore, using Nucleic Acid Based Amplification (NASBA) we demonstrate the utility of the device for bacterial molecular diagnostics using *H. influenzae* as a model organism.

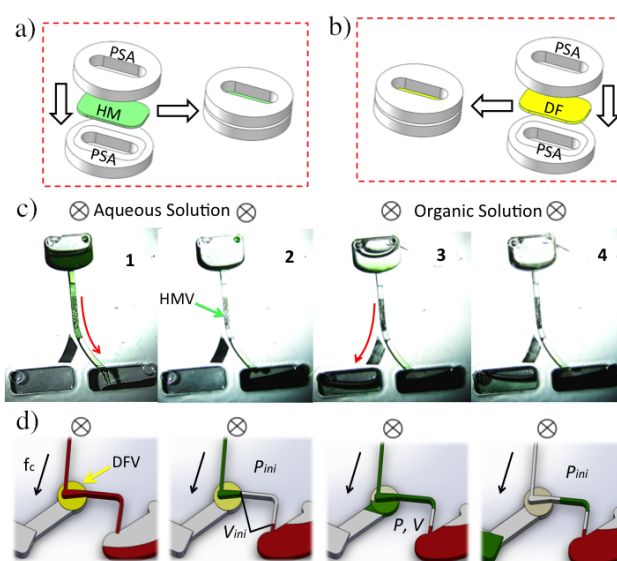


Fig. 1 Routing of flows based on solvent-specific valves in bifurcated microchannels: Assembly of composite tabs for Hydrophobic Membrane (HM, a) and Dissolvable Film (DF, b) valves using Pressure Sensitive Adhesive (PSA). c) Proof of principle for routing of sequentially loaded aqueous (left) and organic (IPA, right) solvents into designated collection chambers using the HM tab in a simple, inverse-Y structure. As the HMV is impermeable to the first aqueous phase, and the flow deflects through the open channel into the right collection chamber (panels 1 and 2). On the contrary, the second (organic) liquid IPA wets the membrane and flows in the left hand-side chamber as the flow resistance of the outlet, governed by the larger cross-section and length of the vertical outlet, is significantly smaller than the flow resistance of the tiny channel leading to the alternative right outlet (panel 3-4). d) Schematic of the fluidic capacitance, dissolution of the DF (yellow), and routing of the aqueous flows, P_{mi} is the atmospheric pressure, V_{mi} is the volume of the lateral channel and P with V are their centrifugally compressed counterparts. The axis of rotation are denoted by \otimes above each panel.

First we demonstrate the underlying principle of solvent-selective routing (Fig. 1). By strategically placing two solvent-selective valve types (Fig. 1a and b) in a simple microfluidic network, inverse-Y bifurcation connecting an inner loading chamber to two outlets (Fig. 1c and d). Within the 3-dimensional (3D) disc architecture similar to an earlier reported system (Gorkin III *et al.*, 2012), we placed the two outgoing channels in separate layers. These channels communicate via a vertical through hole which is initially sealed by a solvent-selective film, in this case a hydrophobic, PTFE supported membrane valve (HMV) (Fig. 1a and c) which becomes permeable upon exposure to organic solvents. As the HMV is impermeable to aqueous solutions, the first aqueous flow is routed through a narrow channel to the right collection chamber (Fig. 1c, 1-2). However, the HMV is permeable for the subsequent organic solution (Fig. 1c, 3-4), which has thus two options for

exiting. The outflow into the left reservoir can be biased by a lower flow resistance, *e.g.* through a shorter connection channel with a larger cross section compared to the other outlet.

In addition, the centrifugally stabilized liquid volume already resident in the right outlet blocks all vents, thus acting akin to a solid plug to practically create a dead-end channel. The system can be simplified because both liquids, *e.g.* aqueous solutions, have identical contact angles with the channel walls and the channel has uniform cross-section on both sides of the air pocket. For the sake of clarity we hence neglect capillary and inertial effects, so the flow into the right outlet will hence stop once the pressure in the interspersed air pocket balances the centrifugal pressure exerted by the incoming liquid.

The air pocket thus acts as a fluidic capacitance (Kim *et al.*, 2008) where the final pressure of the air pocket $P_{ini} \cdot (V_{ini}/V)$ depends on the initial (typically atmospheric) pressure P_{ini} and the ratio of the initial and final volumes V_{ini} and V , respectively (Fig. 1d). The flow in the lateral channel stops once the pressure in the air pocket equilibrates the centrifugally induced pressure $\rho\omega^2\bar{r}\Delta r$ with the liquid density ρ , the angular frequency ω , the radial length \bar{r} and the mean position Δr of the incoming liquid plug. So essentially, the here considered routing function is tightly linked to the sequence of liquids and sealing the air pocket formed between the advancing and the stationary liquids.

We integrate a bench-top method starting with: (i) loading the aqueous lysate, (ii) isopropanol (IPA) mediated RNA precipitation from the aqueous phase, followed by (iii) washing with ethanol (EtOH) and eventual (iv) resuspension of the purified RNA in aqueous buffer. A glass bead solid-phase support is utilized to enhance the purification efficiency of the system. To implement the automated routing of two organic solvents between a first and last aqueous phases, we established a sequence of a HMV and a DF valve (with an interspersed siphon) realized by the tab structures outlined in Fig. 1. The valves were assembled into a tab structure using two pieces of pressure sensitive adhesive (PSA) (Fig. 1a and b). The full router in Fig. 2 displays four chambers for: loading of the solid phase, sample and reagents (chamber L), the aqueous (W_{aq}) and organic waste (W_{org}) and for eluate containing the purified RNA (E_{aq}) in the final step of the solid-phase purification. Within the loading chamber we placed a baffle with laser ablated, 100 μm wide radial grooves (Fig. 2a) to geometrically retain the glass beads ($\leq 106 \mu\text{m}$) under the impact of the centrifugal flow. With its microporous (pore size 0.45 μm) PTFE barrier, the first HMV blocks the aqueous sample and eluate (Fig. 2b, e)

while providing passage of the organic solvents (Fig. 2c, d). These organic phases are both directed to their designated waste (W_{org}), which is the hydrodynamically preferred, axial outlet of the open-channel situation on the centrifugal platform.

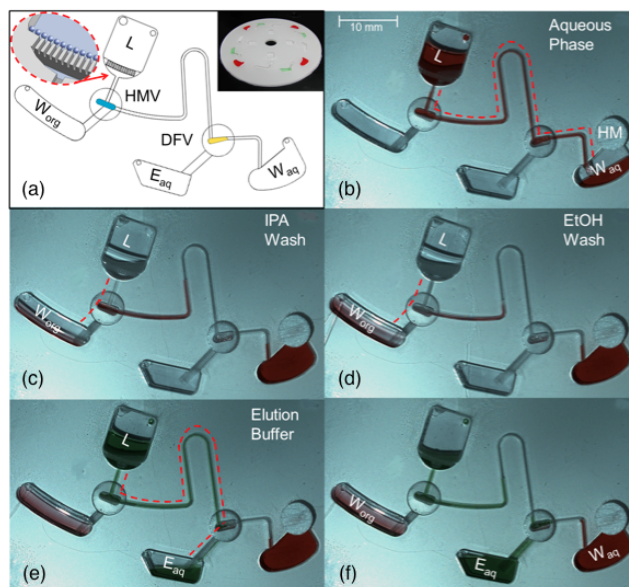


Fig. 2 Fluidic tests of the router. (a) Schematic of the device showing the loading chamber (L), the organic and aqueous waste W_{org} and W_{aq} , respectively, the collection chamber for the eluate E_{aq} containing the purified total RNA and the Hydrophobic Membrane Valve (HMV) and dissolvable film (DFV) valves. The inset on the left shows a magnified view of the baffle that holds the glass beads; the inset on the right shows the assembled disc with the final distribution of liquids; (b) Flow from L designated to W_{aq} . The initially closed DFV is actuated open by the flow. (c) 60 μL of IPA flow from L into W_{org} , as the HMV is permeable to organic solutions. (d) 60 μL of EtOH from L to W_{org} . (e) & (f) Routing of the elution buffer from L into E_{aq} as the HMV is impermeable to water and DFV is open. Summary of this test is available in Online Resource 1. Note that W_{aq} and in particular E_{aq} remain free of organic, which is essential for the quality of the extracted RNA.

The hydrophilic siphon, downstream from the loading chamber, lets the aqueous fraction pass at reduced spin rates, while it holds back subsequent IPA and EtOH before the crest point at increased rates until they are fully diverted into W_{org} . Organic solutions are therefore effectively restricted to the loading chamber, solid phase and ascending siphon arm. The siphon thus minimizes the risk of critical cross-contamination of the elution reservoir E_{aq} with organic solvents. Following this intermediate, organic routing phase, we intersperse a drying period for the previously primed channels and membranes, which could be enhanced by centrifugation (Garcia-Cordero *et al.*, 2010). Again the most crucial factor for a subsequent molecular amplification step is

that E_{aq} remains free of potential contaminants from preceding solutions.

In the final step, the aqueous elution buffer desorbs the RNA bound to the solid phase. After passing the hydrophilic siphon during slow spinning, the RNA depleted sample (Fig. 2b) and the elution buffer (Fig. 2e, f) are diverted in a binary fashion to the aqueous waste (W_{aq}) and the elution chamber (E_{aq}), respectively. To this end a normally-closed (water) dissolvable-film valve (DFV) initially seals the radial outlet to route the liquid into W_{aq} . Once in contact with the valve, the first liquid initiates the timed dissolution of the thin film so the DFV is opened to direct the subsequent elution buffer to its destination E_{aq} . Additionally, the Hydrophobic Membrane (HM) covering the outlet of the aqueous waste (W_{aq}), denoted in Fig. 2b, prevents leakage while venting the chamber. Thus the HM retains the RNA depleted fraction and maintains the air pocket with the advancing aqueous elution buffer. Contact between the two liquids is averted because of the fluid capacitance, i.e. pressure equilibrium on the two sides of the air pocket (Fig. 2e, f). In total, the router utilizes four phase-selective valves (HMF, hydrophilic siphon, DFV and HM) with different functionalities that allow automated sample purification without exposure of the eluted RNA to preceding flows.

The centrifugal microfluidic SPP with this solvent-selective router is based on the following protocol: first, the crude aqueous extract from a homogenized biological sample is introduced onto the beads inside the loading chamber (Fig. 2b). The RNA from the solution binds to the acid-washed glass beads as a result of charge-charge interactions under chaotropic conditions (Boom *et al.*, 1990). Using a specific spin frequency, the RNA-depleted fraction is delivered through the siphon into W_{aq} . The flow disintegrates the thin film so the DFV is open to route the subsequent elution buffer into E_{aq} . Next, the disc is stopped and IPA is pipetted into the loading chamber (L) to precipitate any remaining unbound RNA (Fig. 2c). A small volume of the RNA depleted aqueous solution remains trapped in the channel prior to the siphon crest. Both, its flow resistance and the wettability of the PTFE supported membrane make the HMF impermeable for water, even at high rotational frequencies (75 Hz). As long as the pressure drop across the membrane is lower than the minimum pressure required to drive all of the permeate phase through the membrane (Adamo *et al.*, 2013), the HMF remains closed. Once the IPA is introduced onto disc and is in contact with the HMF pores, it passes through the PTFE supported membrane. According to the supplier, organic solvents, IPA in this case, changes the membrane permeability and thus gates the RNA de-

pleted aqueous solution through the pores of the HMF into the organic waste. The high angular velocity (75 Hz) guarantees that IPA does not shoot over the crest of the siphon, which is a low-frequency pass valve. Such HMF permeability facilitates the emptying of the channel, prior to the siphon crest, into the W_{org} and prevents transfer of the high-salt concentration solution to the elution chamber (E_{aq}). The lost volume does not influence the extraction efficiency as the RNA has been retained on the solid phase prior to the treatment with IPA. It takes approximately 3.5 minutes at spin frequency 75 Hz for the membrane to open as the RNA depleted solution prevents the IPA from direct contact with the HMF. This is the time required for the the IPA to reach the PTFE membrane through the channel at that given spin rate. Using a solvent with higher miscibility would accelerate the processing time. Therefore, the time required to open the HMF is solvent specific, and it also depends on the geometry of the upstream channel, spin rate and intrinsic properties (pore size, contact angle) of the integrated PTFE filter. EtOH is consecutively loaded that rinses away salts from the beads and the precipitated polynucleotides (Fig. 2d), and also residues from the pre-crest channel region. During the drying period, as the EtOH evaporates from the pores of the PTFE supported membrane, the valve returns to its normally closed state. Hence, allows the elution buffer to pass by undisturbed the HMF at low rotational frequencies over the siphon crest into E_{aq} . Finally, 100 μ L of aqueous elution buffer is introduced and driven at at lower frequencies (7.5 Hz) through the solid phase where it retrieves the purified RNA, then past the HMF over the siphon crest and through the now open DFV and vertical channel into the E_{aq} reservoir (Fig. 2e).

3 Materials and methods

Glass beads, acid washed ($\leq 106 \mu\text{m}$), absolute ethanol, isopropanol, Phosphate Buffered Saline (PBS), Pressure Sensitive Adhesive (PSA, Adhesive Research Inc., Ireland), polymethyl methacrylate (PMMA) sheets (Evonik Industries AG, UK), dissolvable film (FA36, Harke Pack-Pro, Germany), hydrophobic membrane (PTFE membrane circles, 0.45- μm pore diameter, Whatman), DI water (TKA, Germany), Nuclease free water (VWR, UK), RNAase ZAP (Biosciences, Ireland), TRI Reagent, 4-bromoanisole (Bio-Science). All reagents listed above were obtained from Sigma-Aldrich unless otherwise stated.

3.1 Valve assembly

These valves were assembled into a tab structure using two pieces of PSA (Fig. 1a, b). First, the flow-through region in a tab was cut out from the PSA using a precision knife cutter (Graphtec, Yokohama, Japan). The protective foil was peeled off the PSA and either a hydrophobic membrane (HM) or a water-dissolvable film (DF) was stacked on the surface (Fig. 1a, b). The excess material was cut off and removed without penetrating the DF layer. A final cut through the PSA defined the tab size. To improve the mechanical stability of the fluid exposed area, a second PSA layer covered the HM/DF at the top.

3.2 Fabrication and assembly of the disc

The device consisted of three PMMA discs ($\phi 120$ mm x $\phi 15$ mm x 1.5 mm) and two binding PSA layers (Fig. 3). Each disc was cut to size and processed on a CO₂ laser (Epilog Zing, US): the bottom disc had its draining channels ablated; in the middle disc liquid loading channels and collection chambers were cut out. Additionally in the middle disc connecting channels, siphons and valve grooves were CNC milled (MDX-40 Roland, UK) into the backside. Inlets and outlet via-holes were ablated in the top disc. All three discs were sonicated in 2% aq. soln. Micro 90 (International Products Corp., US) for 30 min at 50°C. The discs were then transferred in DI water and sonicated under the same conditions for another 30 min. Finally, the discs were heat-dried at 80°C for 45 min.

Prior to disc assembly, the work area on the bench was decontaminated using RNase ZAP and cleaned with 70% IPA. Valves were placed in their designated grooves in the middle disc. Intermittent layers of PSA with the cut out silhouettes (Graphtec, Yokohama, Japan) of all chambers and channels were aligned with their contour parts on the PMMA discs using a bespoke assembly rig. The assembled device was passed multiple times through a roller press (Hot Roll Laminator, Chemsultant Int., US) to reinforce the bonds of the five-layer structure. Finally, 30 mg of acid-washed, dried glass beads was introduced to the loading chamber *L*.

3.3 MCF7 cell culture

All cell culture reagents were obtained from Sigma-Aldrich (MO, USA) unless otherwise stated, MCF7 cells (DSMZ, Braunschweig, Germany) were cultured in 75 cm³ flasks in DMEM media, supplemented with 10% fetal bovine serum (FBS), 100 U mL⁻¹ penicillin and 100

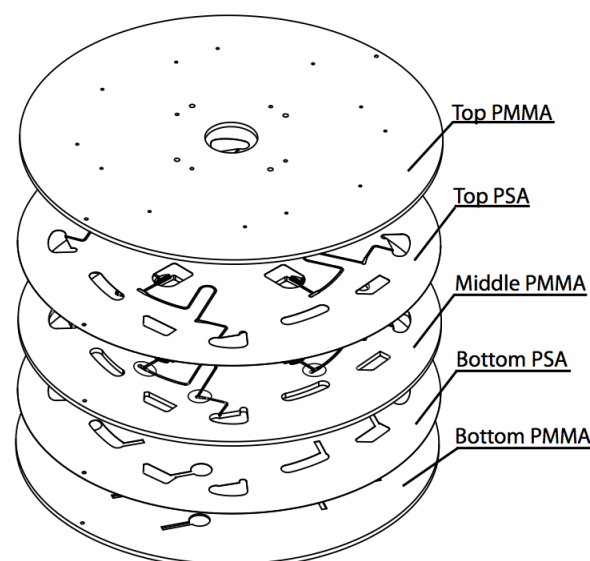


Fig. 3 Exploded view of the disc assembly. The bottom PMMA disc (OD 120 mm x ID 15 mm x 1.5 mm) with laser ablated draining channels was bonded through a bottom pressure sensitive adhesive (86 μ m, PSA) to the middle disc, which hosted the loading, collection chambers, as well as milled channels and valve beds. The channels had uniform square cross-section (0.5 mm x 0.5 mm) and were fabricated by precision milling (MDX40, Roland, UK) on the upper side of the disc. While the valve beds (OD 6 mm, Depth 0.6 mm) were milled from the backside. Top PSA layer with silhouettes of the channels and chambers bonded the stack of to the top PMMA disc, which sealed close the chambers and the channels. Two pins and an assembly rig were used to align all the structures.

μ g mL⁻¹ streptomycin. The cultures were maintained at 37°C with 5% CO₂. Cells were harvested by incubation in 5 mL 0.25% trypsin / 0.1% EDTA at 37°C for 5 minutes followed by neutralization with 5 mL culture medium. Cells were centrifuged at 300 x g for 4 min and resuspended in culture medium. The cells used in this study were collected between their 17 and 25 passages.

3.4 T47D cell culture

The ductal breast cancer (T47D) cells were cultured in RPMI-1640 supplemented with 0.2 U mL⁻¹ bovine insulin and FBS to a final concentration of 10% at 37°C in 5% CO₂. Cells were harvested by incubation in trypsin - EDTA solution at 37°C for 5 minutes followed by neutralization with 5 mL culture medium. Cells were counted, and centrifuged at 300 x g for 4 min to pellet the cells.

3.5 *Haemophilus influenzae* growth conditions

H. influenzae (DSMZ 4690) was cultured overnight in haemophilus test medium (HTM, Oxoid, UK). The following morning, a new culture (10 mL) was inoculated with a 100 μL overnight culture aliquot and allowed to grow to exponential phase (4 hrs). Cells were harvested, the optical density of the culture was measured at 600 nm and compared to a previously generated growth curve. Cells were diluted in HTM to 1×10^7 cells / mL and pelleted.

3.6 Leukocyte preparation

Human whole blood was obtained from a healthy male volunteer. The leukocyte fraction was isolated by gradient density centrifugation using Ficoll paque plus (GE Life Sciences) according to the manufacturers instructions. The cells were washed twice in 1 x PBS and pelleted.

3.7 Bench-top cell lysis and RNA extraction with TRI Reagent

Cells were lysed by mixing a 25 μL aliquot of harvested cells in culture media (DMEM, FBS, penicillin and streptomycin) with 80 μL TRI Reagent. The aliquots contained 2.96×10^5 - 7.4×10^4 MCF7 cells. The cells were enumerated by an automated cell counter (Scepter Handheld, Millipore, US) and in a hematocrit chamber (depth 0.1 mm, Marienfeld, Germany). For all other cell types (T47D, *H. influenzae* and leukocytes), the cell pellet was resuspended in a mixture containing 80 μL TRI Reagent and 25 μL nuclease free water. To each sample, 5 μL of 4-bromoanisole was added. The mixture was then vortexed for 1 min and incubated for 9 min at room temperature prior to purification. All samples were then centrifuged at 14000 x g for 5 min at room temperature and the aqueous phase was removed for on-disc purification.

3.8 Measuring the contact angle between PMMA and aqueous cell homogenate

Following lysis, 60 μL of the aqueous phase was collected, and an equal volume of water was added. From this, a 1- μL aliquot was placed on a clean, dry PMMA surface ($n = 5$) and images of the sitting droplets were acquired. The contact angles were calculated using the tangential method from the built-in software of the goniometer (DataPhysics Instruments GmbH, Germany).

The hydrophilic siphon design (Online Resource 2) was calculated based on this data.

3.9 Bead-based total RNA purification on-disc

The use of silica based substrates in combination with chaotropic salts to purify nucleic acids has been widely implemented (Boom *et al.*, 1990). Under basic and near neutral pH the silanol groups on glass or silica surfaces are negatively charged (Wen *et al.*, 2008) due to their pKa of 5-7. In spite of the pKa, charge-charge interactions can take place in high salt concentration solution. Also, strong ionic conditions (NaCl) and lower pH (pH = 5) can mask native hydroxyl negative charges and permit binding of the RNA. In the protocol we implement here, the chaotropic salt from the TRI reagent compensates the anionic charges by removing water molecules from both glass and nucleotides. To strip the beads of the bound RNA, a low ionic strength buffer at near neutral pH 8.1 is used.

On-disc, 30 mg of dry acid-washed glass beads were introduced into the main chamber. Next, 120 μL of cell lysate mix with water (1:1, aq. phase: water) was loaded. The mixture was incubated for 5 min on a stationary disc to enable RNA binding to the beads. The beads were then subjected to two sequential washing steps with 60 μL of 100% IPA and 60 μL of 75% ethanol aqueous solution (EtOH). Finally, the purified RNA was retrieved from the beads with the addition of 100 μL elution buffer (50 mM Tris-HCl, 1 x EDTA at pH 8.1). The liquids were automatically collected in designated chambers (Fig. 2 and ESM-1). The entire volume of the eluted fraction (100 μL) was recovered from the collection chamber (E_{aq}) and analyzed.

3.10 Measuring the concentration, purity and integrity of extracted RNA

The concentration and integrity of the purified total RNA was determined by capillary electrophoresis (RNA 6000 Pico kit, Bioanalyzer 2100, Agilent technologies, US) according to the manufacturers' instructions. The quality of the purified RNA was assessed by the RIN (RNA Integrity Number) provided by a build-in algorithm of the Agilent Expert Software. The RIN algorithm analyzes the entire electrophoretic trace originating from an RNA sample. First, to determine if RIN could be calculated, depending on important elements of the electropherogram such as the Pre region, 5S region, Fast region, Inter region and Past region are evaluated. If a critical anomaly is detected in any of

these regions, the RIN is not computed. Baseline correction and normalization are automatically applied to each electropherogram prior to the feature extraction. Then, based on Bayesian learning technique, the algorithm builds regression models using indicated peak positions, heights, areas, area ratios, S/N ratio, maximum and minimum values, and waviness of the electropherogram trace to assign a 1 to 10 score (Schroeder *et al.*, 2006). RIN score of 1 means the sample is degraded, and 10 scores for completely intact RNA. According to the description of Agilent, the RIN algorithm is developed to utilize neural networks and adaptive learning in conjunction with a large database of eukaryote total RNA samples, and the RIN score is largely independent of the amount of RNA used and the origin of the sample.

3.11 RT-PCR amplification

The microRNAs, miR-16 and miR-195 were reverse transcribed using miRNA specific stem loop primers (Life Technologies) and the TaqMan[®] MicroRNA reverse transcription kit (Life technologies). 1.33 μL of RT product was subsequently amplified by PCR in a 20 μL reaction using the TaqMan[®] universal PCR master mix II kit and miRNA specific primers and probes (Life Technologies) on a LightCycler 480 thermocycler (Roche).

3.12 NASBA amplification

The tmRNA transcript in RNA purified from *H. influenzae* was amplified in a real time NASBA reaction using the NucliSENS EasyQ basic kit version 2 (bioMérieux, Lyon, France) on a LightCycler 2.0 thermocycler (Roche) using the primers (5-3) P1; AATTCT-AATACGACTCACTATAGGGAGAAGGCTTCGATC-CTCAAACGGT, P2; GCAGCTTAATAACCT and a molecular beacon 5'FAM-CCGAGTGGGGATAACGC-GGAGTCAACTCGG 3'DAB (MWG Eurofins, Germany). Each sample was amplified in a 20 μL reaction consisting of 10 μL of NASBA reagent-primer mix, 5 μL of RNA template, and 5 μL of the enzyme mixture (avian myeloblastosis virus reverse transcriptase, RNase H, and T7 RNA polymerase).

4 Results and discussion

4.1 Fluidic analysis

Liquid volumes, conditions and spin frequencies for each stage of the purification procedure were experimentally

confirmed. The final spin frequency protocol for the purification is outlined in Figure 4. For total RNA, a 5-min incubation period was necessary to enable the beads to bind nucleic acids present in the sample. Another 5-min incubation period was required to provide sufficient time for the RNA to elute from the beads into the aqueous elution buffer in the reverse process. These incubation times and elution conditions relate directly to the properties of the solid phase and may vary for different bead materials, *e.g.* silica (Wen *et al.*, 2008; Duarte *et al.*, 2010) polystyrene (Duarte *et al.*, 2011) or chitosan (Kim *et al.*, 2009b). One advantage of the router presented in this work is that the solid phase inside the loading chamber can be easily substituted, *e.g.* to reduce the incubation times and/or increase the extraction efficiencies.

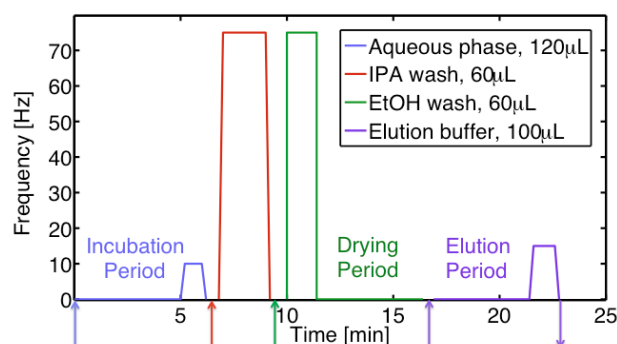


Fig. 4 Spin frequencies of the disc versus time. The vertical arrows on the horizontal axis indicate the four sequential loading steps of sample, reagents and collection of the purified RNA. Simultaneous extraction of total RNA from four samples was accomplished in less than 25 minutes.

It was determined that increasing the period of incubation prior to elution further increased the extraction efficiency. The 5-min drying period (Fig. 4) facilitated the evaporation of any remaining EtOH from the siphon. Drying of the siphon prior to the final elution step resulted in a stabilization of the contact angle thereby preventing elution buffer from seeping over the siphon crest, thus averting the elution buffer from mixing with aqueous waste fraction.

4.2 On-disc RNA purification

To validate proper functioning of the on-disc SPP with the solvent-selective router, we performed lysis and phase separation on the bench of MCF7 cells with TRI Reagent, and subsequent on-disc RNA purification from the aqueous phase obtained from the cell lysate. The electropherograms obtained for different numbers of MCF7

cells in Fig. 5 show that high quality RNA was recovered from the eluted fraction.

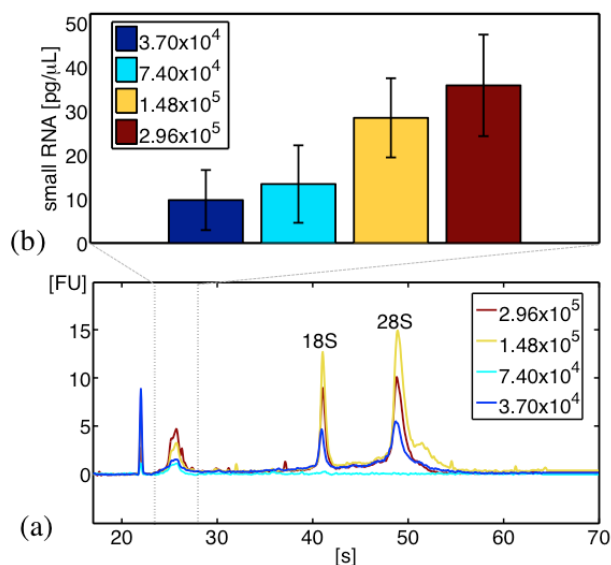


Fig. 5 Electropherogram of the total RNA purified on-disc from four different aliquots of MCF7 cells (a). Vertical lines between 24-28 seconds designate the region of small RNA (size range 30 to 200 nt). (b) Mean values and standard deviations from triplicate samples containing (red) 2.96×10^5 , (yellow) 1.48×10^5 , (light blue) 7.4×10^4 , (blue) 3.7×10^4 of MCF7 cells.

For the MCF7 RNA studied ($n = 8$), RIN values were in the range of 7.2 to 9.2. An average of 16.8 ng was recovered from the 2.96×10^5 cells, which was less than the 23.1 ng from 1.48×10^5 MCF7 cells. Evidently, the cell number and the amount of ribosomal RNA (18S and 28S) are not correlated as indicated by the peak height variations in Fig. 5. We attribute this to the experiments which are performed on different days using asynchronous cells from long-term MCF7 line cultures, implying random fluctuations in gene expression (Hiorns *et al.*, 2004). However, the RIN is the criterion used here to evaluate solid phase extraction and RNA quality on LoaD, which is in the scope of the current article. Based on qualitative analysis of the rRNA we conclude that the purified RNA has preserved high integrity after on-disc purification with the solvent-specific router.

Further analysis indicates that the quantity of recovered small RNAs is proportional to the number of cells in a starting sample. From the integrated area of the peaks with migration time between 24 and 28 seconds, the small RNA fraction was quantified for four different cell concentrations. We focused on this region as many potential biomarkers have been identified as small RNAs (Iorio and Groce, 2012; Kosaka *et*

al., 2010). Figure 5 compares the purified small RNA concentrations to cell content. The results suggest that our LoaD platform is applicable for small RNA purification from acid guanidinium isothiocyanate phenol lysed samples in a quantitative manner.

The purification efficiency was further investigated by comparing the RNA content from the purified (E_{aq}) to the unbound (W_{aq}) fractions. Our quantitative measurements show that the RNA concentration is higher in the purified fraction in comparison to the non-bound, waste fraction. A concentration of $180 \text{ pg } \mu\text{L}^{-1}$ was measured in the purified fraction ($100 \text{ } \mu\text{L}$), against $37 \text{ pg } \mu\text{L}^{-1}$ ($120 \text{ } \mu\text{L}$) in the waste fraction (Fig. 6). These were also compared with the control sample, containing culture media only, where no RNA was detected, demonstrating that the recovered RNA originated from the cells and not from the growth media.

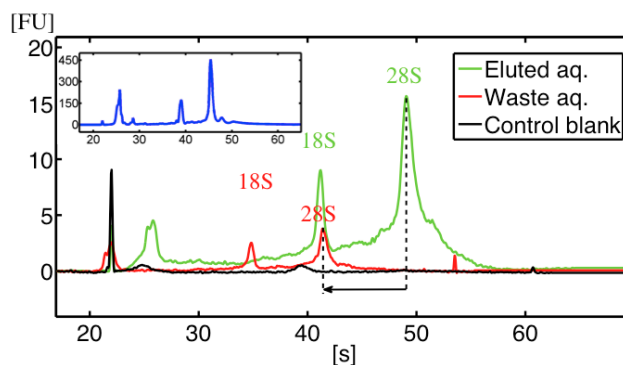


Fig. 6 Electropherograms showing the solid phase extraction efficiency on-disc. Total RNA content was measured (Agilent Bioanalyzer 2100) in samples collected from E_{aq} (green, Fig.2), W_{aq} (red, Fig.2) and control blank from the growth media (black). The spectrum from the waste (red) is significantly shifted to the left in relation to purified RNA spectrum (green), which is due to the increased salt content (inhibiting subsequent molecular amplification) in the W_{aq} . This shift is denoted with dashed lines and an arrow at the ribosomal (28S) peaks. The insert displays the bench-top extracted sample using 2-propanol precipitation and the position of the peaks of pure total RNA (blue).

Literature reports on-chip SPP efficiency for DNA of 42.5% using static silica beads (Duarte *et al.*, 2010). Higher extraction efficiencies of 63.9% are achieved for DNA using dynamic methods with magnetically induced enhanced mixing (Duarte *et al.*, 2011) and 71.0% for RNA utilizing chitosan-coated beads on-chip (Hagan *et al.*, 2009) and recently 81.0% on-disc with (TEOS)-treated glass beads (Seo *et al.*, 2013) to capture RNA from influenza (A H3N2) lysates with known concentrations.

As part of our study, bench-top extraction was performed lysing 9.5×10^4 MCF7 cells, using IPA pre-

precipitation and two consecutive washes with EtOH. We measured total RNA of 32.3 ng from that sample. The RNA recovered from an identical sample after on-disc extraction resulted in 3.9 ng of total RNA. Assuming that the bench-top extraction was 100% efficient, our purification efficiency was 12.1% (weight) of extracted total RNA from an identical sample utilizing a purification protocol without beads. The percentage of purified RNA on-disc varied between samples with different cell counts. For the 1.48×10^5 cells 43% of the total RNA was retained on the beads, from which 7.2% was recovered from the elution fraction. Variations in the packaging of the solid phase would inevitably lead to fluctuations of the amount of recovered total RNA. Even in a tightly packed monolith, diffusion of the RNA molecules would act as a limiting factor. According to the Einstein-Smoluchowski relation for one-dimensional diffusion ($x^2 = 2 \cdot D \cdot t$) during the incubation time (5 min) an RNA molecule with diffusion constant of 10^{-7} cm^2/s , for prokaryotic (16S) ribosomal RNA (Tam *et al.*, 1981), would only travel 7.7 μm . Introducing mixing (Duarte *et al.*, 2011) in the L chamber of the Load system can increase the capture efficiency at the loading stage. Further investigation and optimization of the solid phase extraction protocol should follow in order to further raise both the capture and elution efficiency of total RNA.

A closer look at the electropherogram illustrated in Fig. 6 reveals that the run time of the sample from W_{aq} is increased in relation to the typical migration times. We attribute this behavior to residual salts in the W_{aq} chamber (Copoys *et al.*, 2007).

4.3 Assessment of on-disc RNA purity

To further investigate the presence of contaminants in the eluted fraction, we sought to determine whether salts and/or other contaminants would inhibit enzymatic amplification of RNA species present in the E_{aq} . Nucleic acid modification enzymes and polymerases are inhibited by organic species such as phenol (Katcher and Schwartz, 1994), ethanol (Haggett *et al.*, 2008) and the presence of guanidinium salts. We therefore sought to determine if on-disc purified RNA was amplifiable by RT-PCR and NASBA. For RT-PCR, RNA was purified from the lysate of 1×10^5 T47D cells (Human ductal breast epithelial tumor cell line) and the leukocyte fraction from 1 mL of human whole blood. The microRNAs, miR-195 and miR-16 were first reverse transcribed using a sequence specific primer and then amplified by real-time PCR. The comparison study between the breast cancer related miR-195 and the housekeeping miR-16 after RT-PCR were plotted in Figure 7.

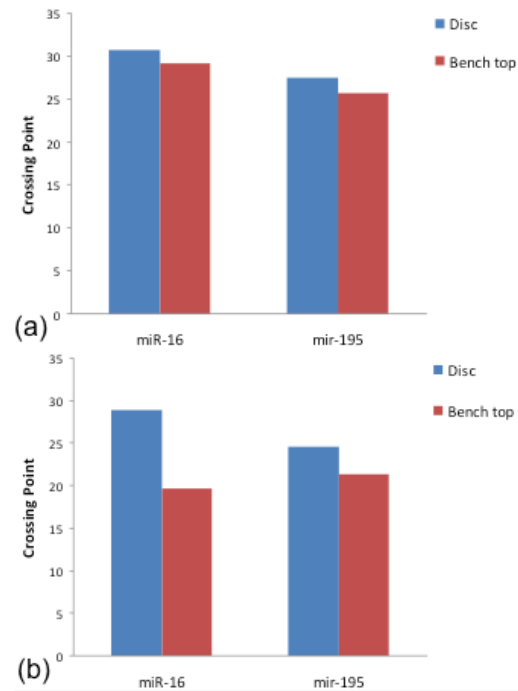


Fig. 7 Comparison study of the RT-PCR amplified miR-16 and miR-195 after on disc or bench top purification. Panel (a) shows the miR-16 and miR-195 purified from 1×10^5 T47D Human ductal breast epithelial tumor cells, and in (b) the leukocyte fraction of 1mL whole blood is presented.

In the RT-PCR the number of cycles needed for the amplification-associated fluorescence to reach a specific threshold level of detection, called crossing point value, is inversely correlated to the amount of nucleic acid found in the original sample (Valasek and Repa, 2005). For the T47D cells, Cp values of 30.6 and 29.1 were obtained for miR-16 with on-disc and bench top purified RNA, respectively. For miR-195, the Cp values were 27.4 and 25.3 for on-disc and bench purified RNA, respectively (Figure 7a). This result indicates an approximately 3-fold reduction in the quantity of both miRNAs detected from disc purified RNA compared to bench purified RNA. In the case of RNA purified from leukocytes, the difference was even greater. For miR-16 there is a 600-fold reduction in the quantity detected (9.2 cycles) and a 9-fold reduction (3.1 cycles) for miR-195. Nonetheless, these results demonstrate that our Load is capable of purifying small RNAs that are amplifiable from two different biological sample types.

One of the main questions in this study was whether the system was capable of purifying RNA from different organism types (human cells and bacteria) that could be later used in various downstream analysis processes. To further address this question, *H. influenzae* cells were lysed, RNA purified on disc, and tested for quality using NASBA amplification. The isothermal nature of

the reaction lends it to point of care diagnostics. Whilst the reaction is isothermal, it does require the simultaneous action of three enzymes to work. Figure 8 indicates that the amount of RNA purified on-disc and amplified is comparable to the bench-top purified RNA. It should also be noted that the tmRNA transcript is 360 bases in length, considerably longer than miRNAs.

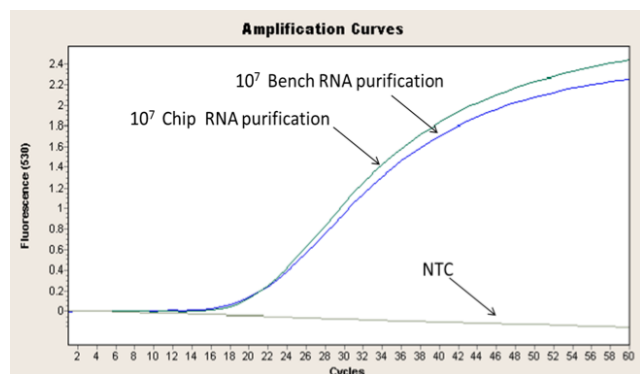


Fig. 8 NASBA amplification of the tmRNA transcript from total RNA purified from *Haemophilus influenzae* (10^7 cells) on-disc and bench-top. Shown in green is the disc purified RNA, blue is the bench purified RNA and gray represents the no template control (NTC).

Preferential retention of tmRNA on disc should correlate to the intrinsic properties of the system and/or the extraction protocol. The literature described (Balladur *et al.*, 1997) adsorption as a three-step mechanism starting with (i) diffusion, in our case with convection, from the solution to the surface, (ii) lateral diffusion on the surface involving rearrangement of adsorbed entities and (iii) adsorption/desorption equilibrium of the molecules at the interface. The observed selectivity during on-disc SPP could be explained in part by the centrifugally induced flux, which forced the liquid through the bead bed in the *L* chamber. At this initial stage of the protocol, time is another factor. Though velocity and contact time contribute to the selective adsorption of tmRNA; in the authors opinion selectivity was mainly governed by desorption. For instance, constant angular velocity under similar experimental conditions resulted in higher recovery of total RNA from MCF7 cells (Kinahan *et al.*, 2014). In the context of reversible binding (iii), it would be more difficult for larger RNA species (18S and 28S), due to their larger hydrodynamic radii, to remain adsorbed on the solid surface under the shear stress resulting from the disc acceleration (Kim *et al.*, 2004) during washing with IPA and EtOH. This finding has important implications for developing Load systems, which target size specific purification of molecules by solid phase purification (SPP).

Despite the limitations in capture and elution during the solid phase purification of total RNA, sufficient quantities and quality of RNA for downstream analysis is retained and recovered utilizing the solvent-selective Load router. These findings further support the feasibility of the router for sample preparations from both prokaryotic and eukaryotic samples.

5 Conclusions and outlook

In summary, we have purified total RNA with high integrity from cell lysates through an automated, merely rotationally actuated flow control strategy involving a network of solvent-selective valves. Purifying mammalian and bacterial RNA, we demonstrated the applicability of the platform did not depend on the source but on the extraction conditions. The high accelerations during the Load purification contributed strongly to desorption and acted as a selective mechanism for the purification of RNA. Under the studied conditions, the shear stress induced by acceleration resulted in an overall low recovery of total RNA. In the future, we seek to improve the total RNA extraction efficiency by using alternative solid-phase materials and by improved packing of the solid phase. The fully automated system will also include Based on the developed extraction platform, we further plan to integrate pre-storage and release of reagents (van Oordt *et al.*, 2013), an upstream chemical cell lysis and the first stage 3-phase liquid-liquid RNA extraction as well as a downstream microarray to provide a sample-to-answer, point-of-care molecular diagnostic device for early diagnostics of breast cancer measuring the expression levels of circulating miRNA molecules, including miR-16.

Acknowledgements This work was supported by the Science Foundation Ireland under grant 10/CE/B1821. Jennifer Gaughran was funded through BioAnalysis and Therapeutics Structured PhD Programme (Bio-AT) by HEA-PRTL V. The authors also thank Prof. Richard O’Kennedy’s group in Dublin City University for allowing us to use their cell culture facilities. We would also like to thank Karsten Holona and her team in Harke PackPro for providing dissolvable films.

References

- Adamo A, Heider PL, Weeranoppanant N, Jensen KF (2013) Membrane-Based, Liquid-Liquid Separator with Integrated Pressure Control. *Industrial Eng Chem Research* 31:10802–808
- Balladur V, Theretz A, Mandrand B (1997) Determination of the Main Forces Driving DNA Oligonucleotide

- Adsorption onto Aminated Silica Wafers. *J Colloid Interface Science* 2:408–18
- Brenner T, Glatzel T, Zengerle R, Ducrée J (2005) Frequency-dependent transversal flow control in centrifugal microfluidics. *Lab Chip* 5:146–50
- Boom R, Sol CJ, Salimanas MM, Jansen CL, Wertheim van Dillen PM, van der Noordaa J (1990) Rapid and simple method for purification of nucleic acids. *J Clin Microb* 28:495–503
- Bustin SA and Nolan T (2004) Pitfalls of Quantitative Real-Time Reverse-Transcription Polymerase Chain Reaction. *J Biomolecular Techniques* 3:155–166
- Cho YK, Lee JG, Park JM, Lee BS, Lee Y, Ko C (2007) One-step pathogen specific DNA extraction from whole blood on a centrifugal microfluidic device. *Lab Chip*, 7:565–73
- Chomczynski P and Sacchi N (1987) Acid three phase phenol-chloroform extraction. *Anal Biochem* 1:156–159
- Clancy E, Glynn B, Reddington K, Smith TJ, Barry T (2012) Culture confirmation of *Listeria monocytogenes* using tmRNA as a diagnostics target. *J Microbiological Methods* 3:427–35
- Copois V, Bibeau F, Bascoul-Mollevi C, Salvetat N, Chalbos P, Bareil C, Candeil L, Fraslon C, Conseiller E, Granci V, Mazière P, Kramar A, Ychou M, Pau B, Martineau P, Molina F, Del Rio M (2007) Impact of RNA degradation on gene expression profiles: assessment of different methods to reliably determine RNA quality. *J Biotech* 127:549–59
- Duarte GRM, Price CW, Littlewood JL, Haverstick DM, Ferrance JP, Carrilho E, Landers JP (2010) Characterization of dynamic solid phase DNA extraction from blood with magnetically controlled silica beads. *Analyst* 135:531–37
- Duarte GRM, Price CW, Augustine BH, Carrilho E, Landers JP (2011) Dynamic solid phase DNA extraction and PCR amplification in polyester-toner based microchip. *Anal. Chem.* 83:5182–89
- Ducrée J, Haeberle S, Lutz S, Pausch S, Stetten FV, Zengerle R (2007) The centrifugal microfluidic Bio-Disk platform *J Micromech Microeng* 17:103–15
- Foudeh AM, Fatanat TD, Veres T, Tabrizian M (2012) Microfluidic designs and techniques using lab-on-a-chip devices for pathogen detection for point-of-care diagnostics. *Lab Chip* 12:3249–66
- Garcia-Cordero JL, Basabe-Desmonts L, Ducrée J, Ricco AJ (2010) Liquid recirculation in microfluidic channels by the interplay of capillary and centrifugal forces. *Microfluidics Nanofluidics* 9:695–703
- Gorkin III R, Nwankire CE, Gaughran J, Zhang J, Donohoe GG, Rock M, O’Kennedy R, Ducrée J (2012) Centrifugo-pneumatic valving utilizing dissolvable films. *Lab Chip* 12:2894–902
- Haeberle S, Pausch S, Burger R, Lutz S, von Stetten JDF, Zengerle R (2007) Automation of nucleic acid extraction by a Coriolis-force actuated droplet router *μTAS Proc.*, 1231–33
- Hagan KA, Meier WL, Ferrance JP, Landers JP (2009) Chitosan-coated silica as a solid phase for RNA purification in a microfluidic device. *Anal Chem* 81:5249–56
- Huggett JF, Novak T, Garson J, Green C, Morris-Jones SD, Miller RF, Zumla A (2008) Differential susceptibility of PCR reactions to inhibitors: an important and unrecognised phenomenon. *BMC Research Notes* 1:70
- Heneghan HM, Miller N, Kelly R, Newell J, Kerin MJ (2010) Systemic miRNA-195 differentiates breast cancer from other malignancies and is a potential biomarker for detecting noninvasive and early stage disease. *Oncologist* 7:673–82
- Hiorns LR, Bradshaw TD, Skeleton LA, Yu Q, Kelland LR, Leyland-Jones B (2004) Variation in RNA expression and genomic DNA content acquired during cell culture. *Brit J Cancer* 90:476–82
- Iorio MV and Croce CM (2012) MicroRNA involvement in human cancer. *Carcinogenesis* 33:1126–33
- Jung JH, Park BH, Choi YK, Seo TS (2013) A microbead incorporated centrifugal sample pretreatment microdevice. *Lab Chip*13:3383–88
- Katcher HL and Schwartz I (1994) A distinctive property of Taq DNA polymerase: enzymatic amplification in the presence of phenol. *Bio Techniques* 1:84–92
- Kim J, Hee Jang S, Jia G, Zoval JV, Da Silva N, Madou MJ (2004) Cell lysis on a microfluidic CD (compact disc). *Lab Chip* 5:516–22
- Kim J, Kido H, Rangel RH, Madou MJ (2008) Passive flow switching valves on a centrifugal microfluidic platform. *Sens Actu B: Chemical* 2:613–621
- Kim J, Johnson M, Hill P, Gale BK (2009) Microfluidic sample preparation: cell lysis and nucleic acid purification. *Integr Biology: Quantitative Bioscience From Nano To Macro*, 1:574–86
- Kinahan DJ, Kearney SM, Dimov N, Glynn MT, Ducrée J (2014) Event-triggered logical flow control for comprehensive process integration of multi-step assays on centrifugal microfluidic platforms. *Lab Chip* doi:10.1039/C4LC00380B
- Kloke A, Fiebach AR, Zhang S, Drechsel L, Niekrawietz S, Hoehl MM, Kneusel R, Panthel K, Steigert J, von Stetten F, Zengerle R, Paust N (2014) The LabTube—a novel microfluidic platform for assay automation in laboratory centrifuges. *Lab Chip*, 9:1527–37

- Kosaka N, Iguchi H, Ochiya T (2010) Circulating microRNA in body fluid: a new potential biomarker for cancer diagnosis and prognosis. *Cancer Science* 101:2087–92
- Lee BS, Lee JN, Park JM, Lee JG, Kim S, Cho YK, (2009) A fully automated immunoassay from whole blood on a disc. *Lab Chip*, 9:1548–55
- Lee BS, Lee YU, Kim HS, Kim TH, Park J, Lee JG, Kim J, Kim H, Lee WG, Cho YK (2011) Fully integrated lab-on-a-disc for simultaneous analysis of biochemistry and immunoassay from whole blood. *Lab Chip*, 11:70–78
- Linares AV, Gorkin III R, Glynn B, Godino N, Miller N, Kerin M, Barry T, Smith TJ, Ducreé J (2011) Purification of miRNA from whole blood by chemical lysis and phase separation in a centrifugo-pneumatic micro-homogenizer μ TAS *Proc.* 1460–62
- Madou MJ, Zoval J, Jia G, Kido H, Kim J, Kim N (2006) Lab on a CD. *Ann Rev Biomed Eng* 8:601–28
- Mark D, Haeberle S, Metz T, Lutz S, Ducreé J, Zengerle R, Stetten FV (2008) Aliquoting Structure for Centrifugal Microfluidics *MEMS Proc* 11–14 (2008).
- McCalla SE and Tripathi A (2011) Microfluidic reactors for diagnostics applications. *Ann Rev Biomed Eng* 13:321–43
- Mitchell PS, Parkin RK, Kroh EM, Fritz BR, Wyman SK, Pogosova-Agadjanian EL, Peterson A, Noteboom J, O'Briant KC, Allen A, Lin DW, Urban N, Drescher CW, Knudsen BS, Stirewalt DL, Gentleman R, Vessella RL, Nelson PS, Martin DB, Tewari M (2008) Circulating microRNAs as stable blood-based markers for cancer detection. *Proc Nat Acad Sci USA* 50:10513–21
- Nwankire CE, Donohoe GG, Zhang X, Siegrist J, Somers M, Kurzbuch D, Monaghan R, Kitsara M, Burger R, Hearty S, Murrell J, Martin C, Rock M, Barret L, Daniels S, McDonagh C, O'Kennedy R, Ducreé J (2013) At-line bioprocess monitoring by immunoassay with rotationally controlled serial siphoning and integrated supercritical angle fluorescence optics. *Anal Chem Acta*, 781:54–62
- O'Grady J, Lacey K, Glynn B, Smith TJ, Barry T, Maher M (2009) tmRNA—a novel high-copy-number RNA diagnostic target—its application for *Staphylococcus aureus* detection using real-time NASBA. *FEMS microbiology letters* 2:218–23
- van Oordt T, Barb Y, Smetana J, Zengerle R, von Stetten F (2013) Miniature stick-packaging - an industrial technology for pre-storage and release of reagents in lab-on-a-chip systems. *Lab Chip* 15:2888–92
- Park JM, Cho YK, Lee BS, Lee JG, Ko C (2007) Multifunctional microvalves control by optical illumination on nanoheaters and its application in centrifugal microfluidic devices. *Lab Chip*, 7:557–64 (2007).
- Park BH, Jung JH, Zhang H, Lee NY, Seo TS (2012) A rotary microsystem for simple, rapid and automatic RNA purification. *Lab Chip*, 12:3875–81
- Park J, Sunkara V, Kim TH, Hwang H, Cho YK (2012) Lab-on-a-disc for fully integrated multiplex immunoassays. *Anal Chem*, 84:2133–40
- Sasagawa Y, Nikaido I, Hayashi T, Danno H, Uno KD, Imai T, Ueda HR (2013) Quartz-Seq: a highly reproducible and sensitive single-cell RNA-Seq reveals non-genetic gene expression heterogeneity. *Genome Biology* 14:R31
- Schembri CT, Burd TL, Kopf-Sill AR, Shea LR, Braynin B (1995) Centrifugation and capillarity integrated into a multiple analyte whole blood analyser. *J Autom Chem* 17:99–104
- Schroeder A, Mueller O, Stoccker S, Salowsky R, Leiber M, Gassmann M, Lightfoot S, Menzel W, Granzow M, Regg T (2006) The RIN: an RNA integrity number for assigning integrity values to RNA measurements. *BMC Molecular Biology* 7:3
- Steigert J, Brenner T, Grumman M, Riegger L, Lutz S, Zengerle R, Ducreé J, (2007) Integrated siphon-based metering and sedimentation of whole blood on a hydrophilic lab-on-a-disk. *Biomed Microdev*, 9:675–79
- Tam MF, Dodd JA, Hill WE (1981) Physical Characteristics of 16S rRNA under Reconstitution Conditions. *J Biol Chemistry* 12:6430–34
- Tan SC and Yiap BC (2009) DNA, RNA, and protein extraction: the past and the present. *J Biomedicine Biotechnology*
- Valasek MA and Repa JJ (2005) The power of real-time PCR. *Adv Physiol Educ* 29:151–159
- Wen J, Legendre L, Bienvenue JM, Landers JP (2008) Purification of nucleic acids in microfluidic devices. *Anal Chem* 80:6472–79
- Zehnle S, Schwemmer F, Roth G, von Stetten F, Zengerle R, Paust N (2012) Centrifugo-dynamic inward pumping of liquids on a centrifugal microfluidic platform. *Lab Chip* 24:5142–45
- Zoval J and Madou MJ (2004) Centrifuge-Based Fluidic Platforms *IEEE Proc* 92:140–53 (2004).